

## High-Speed Lightwave Transmission in Optical Fibers

Herwig Kogelnik

Lightwave technology has become the preferred technology for the transmission of information in an increasing variety of applications. This technology, which is based on lasers and optical fibers, can be used for the transmission of voice, data, and video information in the networks of the local exchange loops; in long-distance trunking; for ca-

is also a multimode fiber technology, but it has its wavelength of operation shifted to the 1.3- $\mu\text{m}$  band, where fiber losses are lower. This technology and the next two generations utilize indium phosphide-based semiconductors for their light sources and detectors. The third generation, which also operates in the 1.3- $\mu\text{m}$  band, marks a shift to single-

---

*Summary.* There has been considerable progress in the telecommunications technology based on the transmission of lightwaves through optical fibers. Systems experiments in the 1.55-micrometer band have now demonstrated the capability of transmitting at rates as high as 2 gigabits per second over fiber lengths exceeding 100 kilometers, without the use of repeaters to boost the signal. Elements of this progress are advances in the fabrication of low-loss single-mode fibers, in the spectral control of semiconductor junction lasers assuring single-frequency operation, and in high-speed detectors and receivers.

---

ble television; in data links; and for computer interconnections. The advantages of this new technology include its high transmission capacity, large repeater spacings, immunity from electromagnetic interference, and the small size and weight of fiber cables. The commercial deployment of lightwave systems is proceeding at a rapid pace, and large systems are under construction in the industrial countries of the world.

Worldwide R&D efforts have rapidly advanced fiber systems through four successive technological generations. The first technology employed multimode fibers, silicon detectors, and gallium arsenide-based lasers or light-emitting diodes operating in the 0.8- $\mu\text{m}$  wavelength band. The second generation

mode fibers, which offer higher transmission capacities. The fourth generation, still in its R&D phase, is a single-mode fiber technology with its operation shifted to the 1.5- $\mu\text{m}$  band, where fiber losses are even lower. At this wavelength, the creation and development of new techniques are required to allow transmission at the desired high bit rates. An example of this is the need for the development of spectrally controlled single-frequency lasers.

The history and fundamentals of lightwave technology, as well as the large diversity of its applications, are thoroughly described in recent textbooks (1-6) and review articles (7-9). Extensive references to and a historical perspective on recent R&D work are given in (8) and (9). In this article I will describe recent R&D efforts aimed at high-capacity transmission at rates of many

gigabits per second over long lengths of fiber (>100 km) without the use of repeaters to boost the signal. I will note the transition to single-mode fibers and to the longer wavelengths, and include a brief discussion of the TAT-8 transatlantic lightwave transmission system. This will be followed by a description of the obstacles posed to high-bit-rate transmission by the chromatic dispersion in fibers, and the advances in single-frequency semiconductor lasers which offer a solution to this problem. Illustrations of progress in high-speed detectors and of experimental high-speed transmission systems conclude the article.

### Low-Loss Single-Mode Fibers

The fibers for present lightwave systems (10) are made of silica glass with the chemical formula  $\text{SiO}_2$ . Dopants such as germania ( $\text{GeO}_2$ ) or fluorine (F) are used to produce small changes of the refractive index of the glass. The fiber core is doped to a higher index than the surrounding cladding to confine the light in the core region by total internal refraction. Single-mode fibers have a core diameter of about 8  $\mu\text{m}$  and core-cladding index differences of a few tenths of a percent. As opposed to the larger core multimode fibers, single-mode fibers allow the light to propagate in only one clearly defined path (or mode). This permits transmission at higher bit rates, because multipath effects which spread the arrival time of a short input pulse are avoided. Extraordinary advances in the understanding and the technology of fiber-making (10) have reduced fiber losses to values which now approach the theoretical limits predicted for  $\text{SiO}_2$ . This includes the requirement for careful control of transition metal and water impurities, which must be reduced to the level of a few parts per billion. A recent accomplishment (11) is shown in Fig. 1, which depicts the measured loss values of a single-mode fiber with a reduced  $\text{GeO}_2$  doping concentration in the core. The latter technique was used to hold scattering losses in the core to a minimum. At a wavelength of 1.57  $\mu\text{m}$  the remarkably low attenuation of 0.157 dB/km was measured. This corresponds to a

---

Herwig Kogelnik is director of the Photonics Research Laboratory, AT&T Bell Laboratories, Holmdel, New Jersey 07733.

light loss of only 4 percent over the distance of 1 km of fiber. Compare this to the 8 percent loss of light that we experience when we look through the clearest of glass windows (due to Fresnel reflection losses at the two window surfaces). Figure 1 also indicates (dashed line) the losses resulting from Rayleigh scattering due to submicroscopic density and composition fluctuations in the glass, and the infrared absorption due to molecular vibrations in the glass lattice. The data in this figure show clearly the low-loss window near 1.3  $\mu\text{m}$  and the region of even lower loss near 1.55  $\mu\text{m}$  in which fourth-generation lightwave systems attempt to operate.

### Long-Wavelength Devices

New semiconductor materials were required to construct reliable lasers and detectors for the low-loss fiber windows at the "long-wavelength" bands near 1.3  $\mu\text{m}$  and 1.5  $\mu\text{m}$ . In the past 10 years, many advances have been made in the search for high-quality substrate materials, for methods of growing the required lattice-matched epitaxial crystal layers, and for the processing of new device structures (8, 9, 12-14). The quaternary material indium gallium arsenide phosphide (InGaAsP), which can be grown lattice-matched on the substrate crystal indium phosphide (InP), has emerged as the dominant material for long-wavelength devices. Figure 2 shows how the band gap energy  $E_g$  of this compound can be tailored by a change in composition (15) where one exchanges indium for gallium content ( $x$ ) and phosphorus for arsenic content ( $y$ ). The corresponding wavelengths are indicated on the right-hand scale. The gallium content is kept to values of approximately  $x = 0.47y$  in order to maintain the lattice match to the InP substrate. The beginning of the scale ( $y = 0$ ) represents InP, and the end of the scale ( $y = 1$ ) corresponds to the compound indium gallium arsenide (InGaAs), which is widely used for long-wavelength photodetectors. By varying the composition, heterostructure lasers have been made to operate at wavelengths from 1.1 to 1.65  $\mu\text{m}$ , a range which conveniently covers the low-loss fiber windows at 1.3 and 1.55  $\mu\text{m}$ .

### The TAT-8 Transatlantic Lightwave System

The TAT-8 transatlantic system (16, 17) is an excellent example of a third-generation single-mode fiber system op-

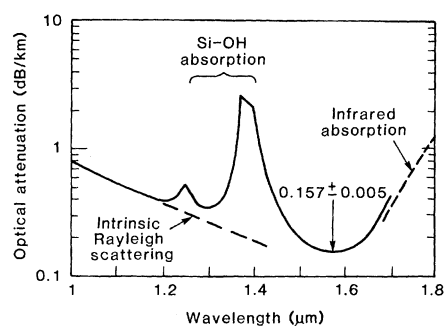


Fig. 1. Optical loss of a low- $\text{GeO}_2$  core single-mode fiber as a function of wavelength. From (11).

erating at a wavelength near 1.3  $\mu\text{m}$ . Construction contracts for this system were awarded to AT&T, Standard Telephone and Cables PLC, and Submarcom in November 1983 with service scheduled for June 1988. Figure 3 shows a map of this system, which will link the United States with Europe through fiber cables totaling 6650 km in length. A branching point is planned at the European continental shelf to allow for transmission to England and France. The AT&T portion of the cable which starts at Tuckerton, New Jersey, contains six single-mode fibers including two spares. The cable design includes steel strands and a copper cylinder to provide the strength needed for laying and recovery operations as well as for sufficient protection from hydrostatic pressure at great sea depths. In order to boost and regenerate the transmitted optical signals under the sea, the system includes about 130 optoelectronic repeaters, which are spaced an average distance of about 50 km. The repeaters contain InGaAsP lasers and InGaAs detectors for each fiber channel,

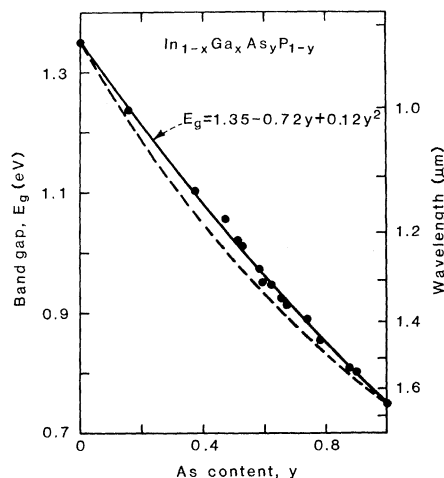


Fig. 2. Band gap energy  $E_g$  of epitaxial InGaAsP compositions, lattice matched to InP, shown as a function of the arsenic content  $y$ . The corresponding laser wavelengths are indicated on the right. From (15).

as well as the necessary repeater electronics. Allowing for spares, this means that more than 1500 lasers will be located under the ocean in the TAT-8 system. The system is expected to operate reliably for a projected life of 25 years.

Like most lightwave systems, TAT-8 is a digital system which transmits information in streams of optical pulses. Each fiber will transmit at a rate of 296 megabits per second (Mb/sec). With voice processing, this will give the system a capacity of about 40,000 two-way voice channels. One gets an idea of the progress that has been accomplished when one compares TAT-8 with the earlier technologies represented by the transatlantic coaxial cable systems. The first coaxial systems, installed in 1955 and 1956, provided a capacity of 48 voice channels with 70-km repeater spacings. The most recent coaxial systems of 1976 and 1983 had a capacity of 4200 voice channels and 9.4-km repeater spacings.

### Pulse Delays in Fibers

Present R&D efforts aim to extend fiber information capacities into the range of multi-gigabits per second, which will require the transmission of very short pulses over long distances. For a better understanding of the issues involved, consider a simple model of the propagation of a pulse of light through a fiber. We know that light propagates in free space with a velocity of about  $c = 3 \times 10^8$  m/sec. In glass, the light velocity is reduced, and we have to make a distinction between the phase velocity  $v_p$  and the group velocity  $v_g$ . The phase velocity indicates the speed at which a node of the sinusoidal carrier wave propagates. It is given by

$$v_p = c/n$$

where  $n$  is the refractive index of the glass. The group velocity describes the speed at which the lightwave carries a pulse envelope. It is given by

$$v_g = c/n_g$$

where  $n_g$  is the group index, which is related to  $n$  and the free-space wavelength  $\lambda$  by

$$n_g = n - \lambda \frac{dn}{d\lambda}$$

The values of  $n$  and  $n_g$  are different because  $n$  changes with  $\lambda$  due to dispersion in the glass.

The propagation delay of an optical pulse transmitted through a fiber of length  $L$  is

$$t_g = L/v_g$$

Fig. 3. Map of the planned transatlantic lightwave system TAT-8. Geographic distances are indicated on the map. The corresponding cable lengths are given in the text.

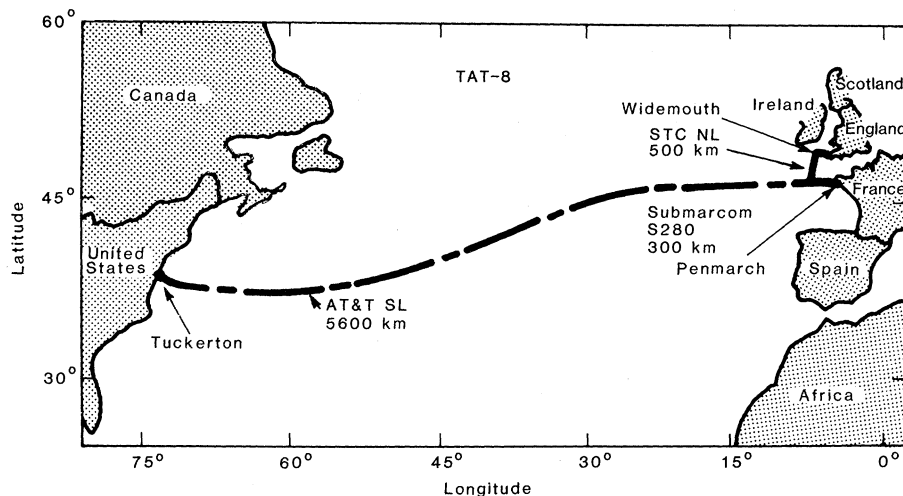
For silica glass,  $n$  and  $n_g$  have values of approximately 1.46. These values lead to a total pulse delay of 0.03 second for the 6350-km stretch of the TAT-8 cable from Tuckerton to Widemouth in England (neglecting delays in the optoelectronic repeaters). By contrast, Fig. 4 shows pulse delay measurements for a short length of fiber ( $L = 7.8$  m) where the pulse delay is only about 40 nsec. These results were obtained by the use of picosecond pulse techniques (18). They show that there are delay differences of tens of picoseconds for pulses of different wavelength. These differences may appear small, but they have very significant implications for high-bit-rate transmission, which is discussed in the following section.

### Chromatic Dispersion in Fibers

Depending on the spectral properties of the laser source and on the kind of modulation employed, a lightwave pulse launched into a fiber contains a set of spectral components of different wavelength. Because of the group velocity dispersion discussed above, these spectral components will travel at slightly different speeds, and will arrive at the fiber output at different times. This will lead to a spreading of a short input pulse, which has to be minimized for high-bit-rate transmission. To estimate this pulse spreading, one uses a measure called chromatic dispersion  $D$ , which is defined as a differential of the group delay  $t_g$  by

$$D = \frac{1}{L} \frac{dt_g}{d\lambda} = \frac{1}{c} \frac{dn_g}{d\lambda} = -\frac{\lambda}{c} \frac{d^2n}{d\lambda^2}$$

This quantity is usually quoted in dimensions of picoseconds of differential delay per nanometer (of wavelength spread) per kilometer (of fiber length). Figure 5 shows data for  $D$  obtained for a single-mode silica fiber. For this particular fiber the dispersion values are only slightly influenced by the dispersion properties of the fiber guide and almost entirely characteristic of the silica glass alone. This is typical of standard fibers (by contrast, the data of Fig. 4 apply to a nonstandard "dispersion-shifted" fiber). In the figure, we note the existence of a zero-dispersion point near  $1.3 \mu\text{m}$ . At this wavelength the lightwave signals propagate faster than at other wavelengths ( $v_g$  is at a maximum) and, more important, pulse spreading due to dispersion is at a minimum.



For readers interested in the physics of materials, it may be interesting to note that the zero-dispersion wavelength  $\lambda_0$  of the material can be simply linked to the average energy gap  $E_0$  of the glass, the electronic oscillator strength  $E_d$ , and the lattice oscillator strength  $E_l$  of the glass (all basic material parameters measured in electron volts). The relation is (19)

$$\lambda_0 = 1.63(E_d/E_0^3 E_l^2)^{1/4} \mu\text{m}$$

For silica glass we have  $\lambda_0 = 1.28 \mu\text{m}$ . This is slightly smaller than the  $\lambda_0$  of  $1.31 \mu\text{m}$  shown in Fig. 5, the difference being due to dopants and guide dispersion. Here it should be noted that special fiber designs are under exploration which deliberately enhance the guide dispersion in order to shift the zero dispersion point to longer wavelengths. This represents

an alternative option for combating the dispersion problem at  $1.5 \mu\text{m}$ .

One obtains an estimate of the dispersive pulse spreading from the spread  $\Delta t_g$  of pulse delay times

$$\Delta t_g = LD\Delta\lambda$$

which is proportional to the fiber length  $L$ , the chromatic dispersion  $D$ , and the spectral spread of the input pulse,  $\Delta\lambda$ . In the low-loss window near  $1.55 \mu\text{m}$ , the dispersion of a conventional single-mode fiber is approximately  $D = 20$  psec/nm·km. The spectral spread of a typical semiconductor laser is about  $\Delta\lambda = 1$  nm or more. With this, one calculates for a fiber length of  $L = 100$  km a pulse spread of  $\Delta t_g = 2$  nsec. This spread is not tolerable in high-speed (multi-gigabits per second) systems, where subnanosecond pulses must be employed. One

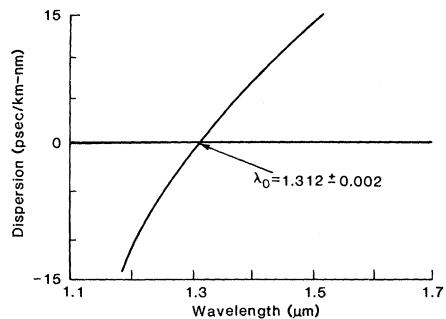
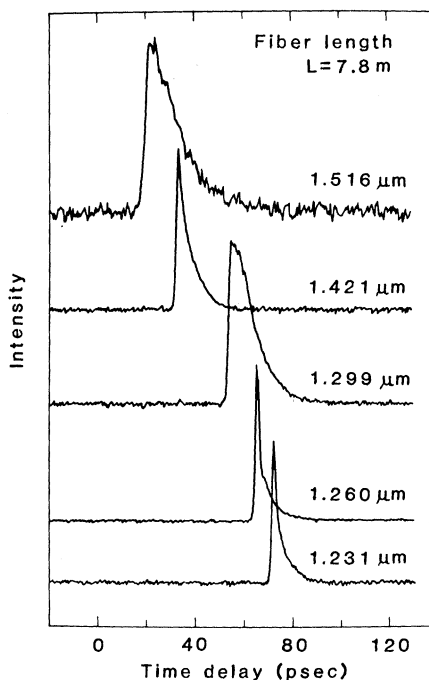


Fig. 4 (left). Picosecond cross-correlation measurement of relative pulse propagation delay for the wavelengths indicated. The fiber length was 7.8 m, and the corresponding total pulse delay was about 40 nsec. From (18). Fig. 5 (right). Chromatic dispersion  $D$  as a function of wavelength for an  $\text{SiO}_2$  single-mode fiber of  $7.5\text{-}\mu\text{m}$  core diameter. From (10).

remedy is the control and reduction of the spectral spread of semiconductor lasers by means of single-frequency laser techniques. This is presently a subject of active research.

### Single-Frequency Lasers

In semiconductor junction lasers the light is amplified by stimulated emission of radiation. This is induced by carrier injection, that is, essentially by passing a current (of a few tens of milliamperes) through the junction. Gain (20, 21) is produced near the wavelength corresponding to the band gap of the semiconductor, as indicated in Fig. 2. Useful gain is available over a spectral band about 30 nm in width. As an illustration, a measurement of the spectral gain dependence for a particular quaternary laser with arsenic content of  $y = 0.6$  is shown in Fig. 6.

Laser oscillation is achieved because the amplified light is reflected back and forth between the mirror-like end facets of the laser crystal. The end facets are typically spaced a distance of  $d = 250 \mu\text{m}$  apart and form a resonant cavity. The frequency of oscillation of a light-wave generated by a junction laser at a wavelength near  $1.5 \mu\text{m}$  is  $\nu = c/\lambda = 2 \times 10^{14}$  cycles per second. Figure 7 depicts the multifrequency output spectrum of a typical junction laser, which contains several spectral lines spread over a wavelength band of about 10 nm. The lines correspond to the resonances of the laser cavity, which are supplied with sufficient gain to oscillate. The frequency spacing  $\Delta\nu$  between the lines is simply the inverse of the round-trip delay time  $t_g$  of a light pulse shuttling back and forth between the laser facets,

$$\Delta\nu = 1/t_g = v_g/2d$$

which corresponds to a wavelength spacing of

$$\Delta\lambda = \lambda^2/2n_g d$$

Here  $n_g$  is the group index and  $v_g$  the group velocity in the semiconductor material (for InGaAsP lasers,  $n_g$  is 3.9 and 3.7 at 1.3 and  $1.55 \mu\text{m}$ , respectively). The wavelength spacing in Fig. 7 is  $\Delta\lambda = 1.25 \text{ nm}$ , from which one calculates a round-trip delay time between the facets of  $t_g = 6.5 \text{ psec}$ .

The objective of single-frequency laser structures is to suppress oscillations at all resonances of the laser but one. An example of a single-frequency laser spectrum is shown in the lower part of Fig. 7. Spectral control techniques of this kind

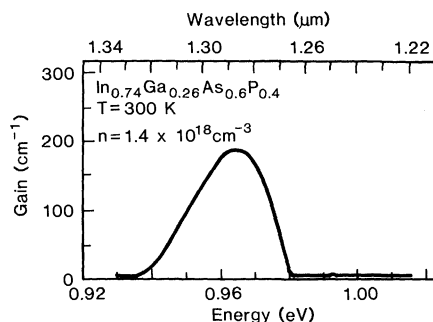


Fig. 6. Spectral dependence of semiconductor laser gain for a carrier density of  $1.4 \times 10^{18} \text{ cm}^{-3}$  at room temperature. The horizontal scales indicate the wavelengths and photon energies. From (20).

have been actively explored in the research laboratories and many advances have been made in the understanding and the technology of single-frequency lasers. Recently, particular attention has been paid to coupled-cavity lasers (22–27) and distributed feedback lasers (28–38).

In the coupled-cavity technique, two junction laser cavities possessing resonances with different spacings  $\Delta\lambda$  are coupled to form one laser structure. Only one of the resonances of each cavity is made to coincide in frequency with a resonance in the other cavity, and this determines the frequency at which the laser is allowed to oscillate.

In distributed feedback lasers the thickness of the lightguide guiding the

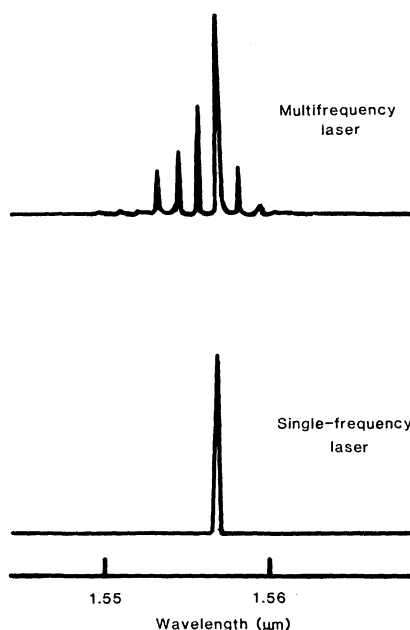


Fig. 7. Output spectrum of a typical junction laser showing multifrequency output and the spectrum of a single-frequency laser. From (27).

radiation through the laser is corrugated in the form of a high-resolution grating. This is sketched in Fig. 8. For operation at  $1.55 \mu\text{m}$ , the corrugations of a first-order grating have a period of about 230 nm, and those of a second-order grating have a period of 460 nm (both first-order and second-order techniques have been used). In this technique Bragg reflection from the grating is used as a feedback mechanism, taking the place of the mirror reflections in standard lasers. The frequency selectivity of the Bragg effect helps to select one frequency of operation. Much progress has been made in mastering the difficult technology of etching the ultrafine corrugations into the semiconductor and in overgrowing these corrugations with high-quality crystal material. Various experimental types of distributed feedback (DFB) lasers are now available in research laboratories.

The system requirements on single-frequency lasers are many. This includes reliability and the requirement that sufficient power levels (milliwatts) be available during single-frequency operation. Another requirement is that a controlled single-frequency spectrum be maintained during high-speed modulation of the laser, where the output light level is modulated through varying the drive current of the laser. Even an occasional jumping of the laser frequency to a neighboring cavity resonance is undesirable because of the low bit-error-rates (of order  $10^{-10}$ ) that are required in transmission systems.

For high-speed transmission, one must pay attention to yet another spectral defect that occurs even when the laser oscillation is restricted to one single resonance  $\nu$ . This defect is called "chirping." It occurs because the refractive index  $n$  in the semiconductor changes by small amounts as a consequence of carrier injection (39). When the modulation current induces an index change  $\delta n$ , then the cavity resonance (and thereby the output frequency) is swept (or chirped) by an amount  $\delta\nu$  according to

$$\delta\nu/n_g = -\delta\nu/\nu = \delta\lambda/\lambda$$

where  $\delta\lambda$  is the corresponding chirp in wavelength. To keep dispersive pulse broadening small, this chirp must be kept to a minimum. In the experiment at 2 Gb/sec to be mentioned below, a special DFB laser (38) was used where the chirp was kept to  $\delta\lambda \approx 0.03 \text{ nm}$ , which corresponds to induced index changes of about  $\delta n = 10^{-4}$  (for InGaAsP lasers  $n = 3.52$  at  $1.3 \mu\text{m}$  and  $n = 3.55$  at  $1.55 \mu\text{m}$ ).

## High-Speed Detectors

The recent advances in fibers and lasers have been accompanied by considerable progress in lightwave detectors suitable for operation at high speeds and in the long-wavelength range. This may be illustrated by a new avalanche photodetector (APD) structure which was successfully used in recent transmission experiments (40). A sketch of this APD is shown in Fig. 9. It consists of a set of crystal layers, each with a different function. The narrow-gap InGaAs layer serves to absorb the light incident through the substrate. The wide-band gap *n*-type InP region amplifies the signal by carrier multiplication. The two regions are designed to be different materials in order to minimize the generation of excess noise during the multiplication process. Between these two layers is a grading layer of intermediate-gap InGaAsP material, which serves to reduce the trapping of carriers (holes) at the InP/InGaAs interface. This trapping would impair the high-speed response of the detector.

This so-called SAGM (separate absorption, grading, and multiplication layers) structure has been optimized to provide simultaneously low noise, high speed, and avalanche multiplication at sufficient gain. In order to achieve these characteristics, careful control is required on the thicknesses and doping levels of the *n*-type layers. Experimental devices have successfully operated in the research laboratory and sensitivities of  $-43$  dBm at 420 Mb/sec and  $-36.6$  dBm at 2 Gb/sec were measured at a wavelength of  $1.55 \mu\text{m}$  (the negative dBm measure indicates light levels in terms of decibels below 1 mW). These sensitivities have allowed the transmission of high-bit-rate signals over long distances.

## High-Speed Transmission Experiments

Transmission experiments explore the limits of a new technology. They serve as a critical test for fibers and for individual components, and they evaluate the interplay of all components in system architectures of interest. For these tests one employs streams of binary pulse signals which represent information in terms of ones and zeroes. After transmission, the received output is compared to the input signals, and errors are counted. Transmission systems require bit error rates (BER) of the order of  $10^{-10}$ . I will mention here two transmission ex-

periments designed to test fourth-generation technology operating at  $1.55 \mu\text{m}$ . Both experiments used low-germanium fibers, DFB lasers, and the new SAGM avalanche detectors to achieve transmission without repeaters over long fiber lengths at high speeds.

In the first experiment (41), signals were transmitted at a rate of 420 Mb/sec over a fiber length of 203 km without repeaters. The BER was better than

$10^{-9}$ . The total fiber loss, including splices, was 41.4 dB. The DFB laser used here had an "overgrown ridge-waveguide" structure (37), had excellent suppression of side resonance frequencies, and exhibited a chirp range of 0.12 nm.

The second experiment (42) was conducted with a transmission rate of 2 Gb/sec over a fiber span of 130 km. A schematic of this experiment is shown in

Fig. 8. Sketch of the cross section of a semiconductor distributed feedback laser. From (38). The composition of the epitaxial layers is designed to confine both the charge carriers and the lightwave.

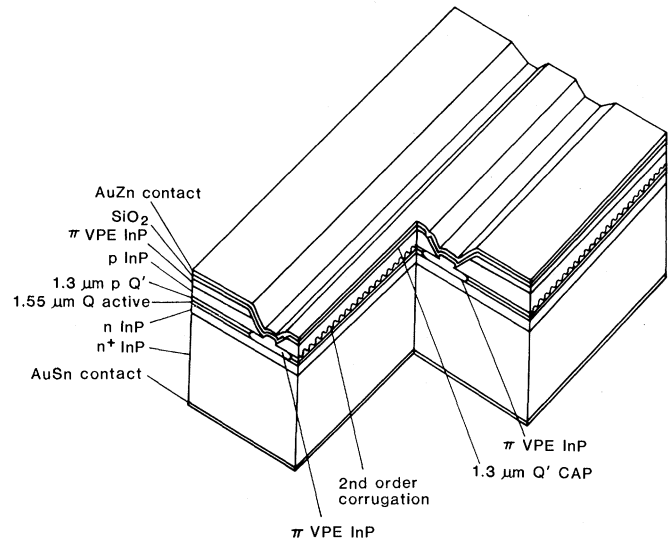


Fig. 9. Schematic cross section of the epitaxial heterostructure layers of an InGaAsP avalanche photodetector. The InGaAsP grading layer is emphasized in black. From (40).

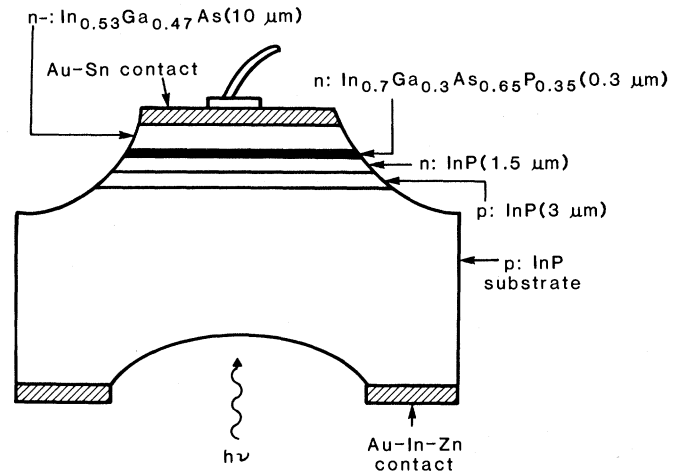


Fig. 10. Schematic of 2-Gb/sec transmission experiment using a DFB laser, a low-germanium fiber, and a SAGM APD receiver with a low-capacitance GaAs field effect transistor amplifier. From (42).

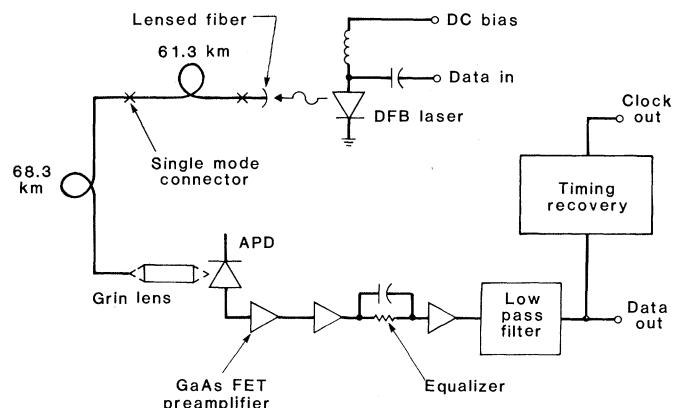


Fig. 10. The laser employed here was a "vapour phase transported" DFB laser (38) with a low chirp of 0.03 nm. The loss of the fiber was 28.3 dB including splices. The receiver had a SAGM avalanche detector and a high-speed low-capacitance design employing GaAs field effect transistors. The bit error rates measured as a function of received power levels are shown in Fig. 11. Again, BER's better than  $10^{-9}$  were demonstrated.

The technology described above is now in the research stage and not yet fully developed and engineered. However, it is a good illustration of the progress of lightwave technology to compare the mentioned results with modern coaxial cable technology. A recent example of this is the so-called T4M digital coaxial cable system. This system has 0.375-inch coaxial cable and transmits at speeds of 274 Mb/sec. The nominal repeater spacing for T4M is 1 mile. Compared to this, the new lightwave technology promises an order of magnitude improvement in transmission capacity, together with a two-order magnitude increase in repeater spacing.

### Concluding Remarks

The rapid development of lightwave technology is underscored by a selection of events which occurred after this article was accepted for publication. The first was an announcement of plans of the Nippon Telegraph and Telephone Public Corporation to construct a trans-Japan single-mode fiber system with a projected total route length of 7000 km. This system will use third-generation technology operating at 1.3  $\mu\text{m}$  with a bit rate of 400 Mb/sec. It will include the Fukuoka-Hiroshima-Osaka-Nagoya-Tokyo-Sendai-Sapporo route, which totals 3000 km in length and which was placed in commercial service in February 1985. Another important event occurred in November 1984, when AT&T announced that it will add 6800 km of new single-mode fiber routes to its terrestrial U.S. lightwave network by 1987, making a projected total of 15,000 km of lightwave routes for that year. Third-

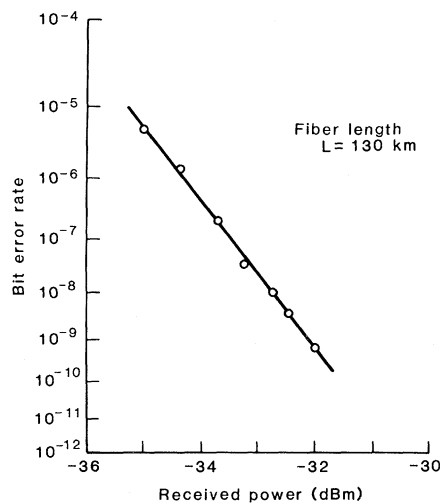


Fig. 11. Bit error rate measured as a function of received power for signals transmitted at 2 Gb/sec for a fiber length without repeaters of 130 km. From (42).

generation 1.3- $\mu\text{m}$  technology will be used with an initial bit rate of 417 Mb/sec and a planned upgrade in later years to 1.7 Gb/sec. Including undersea routes in the Atlantic and Pacific, the company expects to have 34,000 km of lightwave routes in service by the end of this decade. Finally, I should mention two very recent breakthroughs in the research laboratory (43, 44) which have demonstrated lightwave transmission at 4 Gb/sec over fiber distances exceeding 100 km. These experimental systems, operating at 1.55  $\mu\text{m}$ , used further improvements of the fourth-generation technology described in the text. The increased 4 Gb/sec bit rate represents a capacity of more than 50,000 digital voice channels per fiber.

The rate of recent progress has greatly raised expectations for continued advances in lightwave science and technology. The fundamental limits predicted by the physics of photonics materials, devices, and systems have not yet been approached. The challenge of future R&D is an even fuller exploitation of the ultimate capacity of optical fibers.

### References and Notes

1. S. E. Miller and A. G. Chynoweth, *Optical Fiber Telecommunications* (Academic Press, New York, 1979).
2. J. E. Midwinter, *Optical Fibers for Transmission* (Wiley, New York, 1979).

3. S. D. Personick, *Optical Fiber Transmission Systems* (Plenum, New York, 1981).
4. Y. Suematsu, Ed., *Optical Devices and Fibers* (North-Holland, Amsterdam, 1982).
5. C. K. Kao, *Optical Fiber Systems* (McGraw-Hill, New York, 1982).
6. T. Okoshi, *Optical Fibers* (Academic Press, New York, 1982).
7. S. E. Miller, *Science* **195**, 1211 (1977).
8. Y. Suematsu, *Proc. IEEE* **71**, 692 (1983).
9. T. Li, *IEEE J. Selected Areas Commun.* **1**, 356 (1983).
10. P. D. Lazay and A. D. Pearson, *IEEE J. Quantum Electron.* **18**, 504 (1982).
11. R. Csencsits, P. J. Lemaire, W. A. Reed, D. S. Shenk, K. L. Walker, *Proc. Opt. Fiber Commun. Conf., New Orleans* (1984), p. 54.
12. H. Kressel and T. K. Butler, *Semiconductor Lasers and Heterojunction LEDs* (Academic Press, New York, 1977).
13. H. C. Casey, Jr., and M. B. Panish, *Heterostructure Lasers* (Academic Press, New York, 1978).
14. T. P. Pearsall, Ed., *GaInAsP Alloy Semiconductors* (Wiley, New York, 1982).
15. R. E. Nahory, M. A. Pollack, W. D. Johnston, Jr., R. L. Barns, *Appl. Phys. Lett.* **33**, 659 (1978).
16. P. K. Runge and P. R. Trischitta, *Telephony* (23 August 1982), p. 32.
17. Special issue on Undersea Lightwave Systems, *IEEE J. Lightwave Tech.* **2** (December 1984).
18. J. M. Wiesenfeld and J. Stone, *ibid.* **2**, 464 (1984).
19. S. H. Wemple, *Appl. Opt.* **18**, 31 (1979).
20. E. O. Gobel, in (14), p. 313.
21. N. K. Dutta and R. J. Nelson, *IEEE J. Quantum Electron.* **18**, 44 (1982).
22. W.-T. Tsang, N. A. Olsson, R. A. Logan, *Appl. Phys. Lett.* **42**, 650 (1983).
23. C. Lin et al., *Electron. Lett.* **19**, 784 (1983).
24. I. P. Kaminow, J. S. Ko, R. A. Linke, L. W. Stultz, *ibid.*, p. 784.
25. L. A. Coldren, T. L. Koch, C. A. Burrus, R. G. Swartz, *ibid.* **20**, 350 (1984).
26. J. E. Bowers, J. E. Bjorkholm, C. A. Burrus, L. A. Coldren, B. R. Hemenway, D. P. Wilt, *Appl. Phys. Lett.* **44**, 821 (1984).
27. K. Y. Liou et al., *ibid.* **45**, 729 (1984).
28. H. Okuda, Y. Hisayama, J. Kinoshita, H. Furuyama, Y. Uematsu, *Electron. Lett.* **19**, 941 (1983).
29. K. Sehartedjo, N. Eda, K. Furuya, Y. Suematsu, F. Koyama, T. Tanbun-ek, *ibid.* **20**, 80 (1984).
30. K. Utaha, S. Akiba, K. Sakai, Y. Matsushima, *IEEE J. Quantum Electron.* **20**, 236 (1984).
31. Y. Itaya, T. Matsuoka, K. Kuroiwa, T. Ikegami, *ibid.*, p. 230.
32. I. Mito, M. Kitamura, M. Yamaguchi, K. Kobayashi, I. Takano, *ibid.*, p. 261.
33. M. Yamaguchi, M. Kitamura, I. Mito, S. Murata, K. Kobayashi, *ibid.*, p. 233.
34. L. D. Westbrook, A. W. Nelson, P. J. Fiddyment, J. S. Evans, *ibid.*, p. 225.
35. T. Watanabe, S. Suzuki, H. Katsuda, K. Takahashi, T. Nomura, T. Shimen, H. Osanai, *Proc. 9th IEEE Int. Semicond. Laser Conf., Rio de Janeiro* (1984), p. 68.
36. S. Tsuji et al., *ibid.*, p. 12.
37. W.-T. Tsang, N. A. Olsson, R. A. Logan, L. F. Johnson, C. H. Henry, *Appl. Phys. Lett.* **45**, 1272 (1984).
38. T. L. Koch et al., *Proc. 9th IEEE Int. Semicond. Laser Conf., Rio de Janeiro* (1984), paper PD-N-7.
39. C. H. Henry, R. A. Logan, K. A. Bertness, *J. Appl. Phys.* **52**, 4457 (1981).
40. J. C. Campbell, A. G. Dentai, W. S. Holden, B. L. Kasper, *Electron. Lett.* **19**, 818 (1983).
41. V. J. Mazurczyk et al., *Proc. Eur. Conf. Opt. Commun., Stuttgart* (1984), paper PD-7.
42. B. L. Kasper et al., *ibid.*, paper PD-6.
43. A. H. Gnauck et al., *Proc. Conf. Opt. Fiber Commun., San Diego, Calif.* (11-13 February 1985), paper PD2-1.
44. S. K. Korotky et al., *ibid.*, paper PD1-1.